

Heating of a dense plasma by an ultrashort laser pulse in the anomalous skin-effect regime

A. A. Andreev, E. G. Gamaliĭ, V. N. Novikov, A. N. Semakhin, and V. T. Tikhonchuk

P. N. Lebedev Physics Institute, Russian Academy of Sciences

(Submitted 12 December 1992)

Zh. Eksp. Teor. Fiz. **101**, 1808–1825 (June 1992)

The absorption of laser light in an overdense plasma with a sharp boundary and the heating of the plasma under conditions corresponding to the anomalous skin effect are studied. Heat transfer from the absorption region near the surface into the interior of the plasma is studied in the kinetic approximation. At high intensities of the laser pulse, the electron distribution function is deformed, and the plasma is heated at a rate tens of times that predicted by classical heat-transfer theory, because of the severe limitation on thermal conductivity. The anisotropy of the electron distribution function in the skin layer leads to an increase in the absorption coefficient. The angular distribution and the polarization dependence of the absorption coefficient are discussed.

1. INTRODUCTION

Since laser pulses of ultrashort length (less than 1 ps) and extremely high power (above 10 TW) have become available, much interest has been attracted to the use of these pulses to produce plasmas and to heat them to high temperatures. A qualitatively distinguishing feature of such short pulses is seen in their interaction with condensed targets, in which case a plasma with an electron density up to 10^{24} cm^{-3} arises in the surface layer. The laser pulse is so short that the ions are effectively immobile. The plasma boundary is therefore sharp, and the radiant energy is transferred exclusively to the electrons. In this regard, the case of subpicosecond pulses differs from the case (which has received more study) in which nanosecond laser pulses are applied to a target. In that case, the outflow of plasma results in the formation of a smooth density profile, with a length scale greater than the laser wavelength. The energy is deposited in a comparatively low-density plasma, with an electron density below the critical value

$$n_c = m\omega_0^2 / 4\pi e^2 = 10^{21} \text{ cm}^{-3} / \lambda_{mkm}^2$$

(m and e are the mass and charge of an electron, ω_0 is the laser frequency, and λ_{mkm} is the laser wavelength in microns). Because of this distinguishing feature of subpicosecond laser pulses, one would expect that plasmas of high density and simultaneously high temperature could be produced by them.¹ Such a capability might prove useful in several practical applications. It would also be of independent interest for research on the behavior of matter under extreme conditions.

In experiments currently being carried out, plasmas with electron temperatures up to 300 eV are produced at laser pulse intensities up to 10^{14} – 10^{15} W/cm^2 and at laser pulse lengths of 0.3–0.5 ps (Refs. 2–5). The energy is absorbed under normal-skin-effect conditions, with the electron mean free path shorter than the depth to which the field penetrates into the plasma. Theoretical estimates^{1,6,7} indicate that it would be possible to raise the plasma heating rate substantially at high intensities of the laser pulse, such that anomalous-skin-effect conditions hold. Because of the collisionless nature of the absorption and the nonclassical energy transport in the plasma, some distinctly nonlinear effects might be seen.

In this paper we are reporting a study of the absorption of light and of plasma heating under anomalous-skin-effect conditions. We will first discuss the heating of a plasma on which the laser light is incident normally. The heating rate is determined by a balance struck between the rate of energy deposition (which is determined by the absorption coefficient) and the rate at which energy is lost from the absorption region (primarily because of electron thermal conductivity). Because of the collisionless nature of the electron motion near the absorption region, the heat transfer should in general be described kinetically. Noting that the skin layer is thin in comparison with the electron mean free path, and noting the results of Refs. 6 and 7, we describe the absorption of the laser light by means of a special type of boundary condition on the electron distribution function in a semi-infinite plasma. This approach simplifies the analysis of the heating process, since it does not require a detailed description of the electron distribution function at the scale of the skin thickness. This approach is particularly convenient for a numerical solution of the corresponding kinetic equation, since the latter equation does not contain the electromagnetic scale.

The results of the numerical solution of the kinetic equation which are reported below will be compared with estimates of the heating rate found previously in the case in which there is absolutely no loss^{1,6} (a maximum estimate) and in the case of a classical (collisional) thermal conductivity⁷ (a minimum estimate). We will see that the electrons acquire a non-Maxwellian anisotropic distribution function in the course of the heating. The heat flux turns out to be well below the classical value, and the calculated heating rate exceeds the minimum estimate by a factor of tens.

The development of an anisotropic distribution function during the heating has served as the starting point for a further study of the absorption of the laser light. This absorption, in a dense plasma under the conditions corresponding to the anomalous skin effect, is studied as a function of the distribution function, the angle of incidence of the laser light, and the polarization of this light. We find that anisotropy can approximately double the absorption coefficient in the case of normal incidence, and it can lead to essentially total absorption of p -polarized laser light at certain angles of incidence.

2. KINETIC CALCULATIONS ON THE DYNAMICS OF PLASMA HEATING UNDER CONDITIONS CORRESPONDING TO THE ANOMALOUS SKIN EFFECT, WITH LIGHT INCIDENT NORMALLY

2.1. Analytic solutions

When laser pulses, even relativistically intense pulses, are applied to condensed targets, the time scale of the plasma heating is greater than the period of the laser wave, and the energy acquired in one event of an interaction with the field is smaller than the oscillation energy in this field.¹⁸ The absorption of laser energy can thus be described by perturbation theory. The change caused in the distribution function by the light is assumed to be small in comparison with the main part of the distribution function, which is formed over a time much longer than the period of the laser light. The absorption coefficient can then be expressed in terms of the main part of the distribution function, which is generally unknown at the outset and must be determined in a self-consistent fashion, with allowance for the energy deposition and the energy loss from the skin layer. Only after we have determined this main part of the distribution function can we calculate the plasma heating rate.

A maximum estimate of the heating rate was found in Refs. 1 and 6 under the assumption that there is absolutely no loss of heat from the skin layer. All the absorbed laser energy was assumed to be transferred to the electrons of the skin layer, and the average energy $\langle \epsilon_e \rangle$ of these electrons was assumed to increase in direct proportion to the heating time t (Ref. 1):

$$\langle \epsilon_e \rangle \approx (E_0^2 / 8\pi n_e) \omega_0 t. \quad (1)$$

There is also an increase in the depth of the skin layer, $l_S \propto t^{1/6}$. Here E_0 is the electric field amplitude of the laser light in vacuum, ω_0 is the frequency of this light, and n_e is the electron density of the plasma.

As the heating proceeds, the distribution function becomes deformed. It deviates from a Maxwellian distribution in being deficient in slow and fast particles. A self-similar isotropic distribution function was derived in Ref. 6:

$$f_e(v) = (9b^2 / 4\pi \langle v \rangle^3) (v / \langle v \rangle) \exp(-bv^3 / \langle v \rangle^3). \quad (2)$$

where $\langle v \rangle = (2\langle \epsilon_e \rangle / m)^{1/2} t^{1/2}$, and $b = [\Gamma(\frac{1}{3})]^{-3/2}$. Figure 1 shows a plot of function (2), which has been normalized by $\int dv f_e(v) = 1$. Shown for comparison by the dashed line is a Maxwellian function. Note that the derivative is positive at low velocities. This positive derivative may be responsible for a secondary instability of the electrons in the skin layer. In particular, it might lead to the excitation of ion acoustic turbulence.²⁰ However, we will not discuss that effect in this paper.

The assumption that there is no loss from the skin layer leads to a maximum estimate of the plasma heating rate. This maximum estimate is not attainable in practice. To find a minimum estimate of the heating rate we can assume that the heat flux out of the skin layer is described by the classical heat-conduction equation. As we know, the classical formulas correspond to the maximum heat flux and thus the minimum heating rate which are possible for the given plasma parameter values. A self-similar solution of the problem of the heating of a plasma with a classical thermal conductivity was derived in Ref. 7. It follows from that solution that the

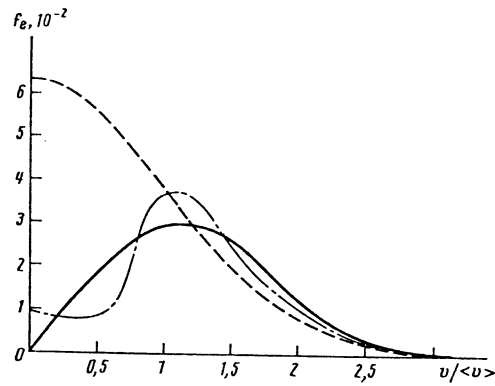


FIG. 1. Normalized electron distribution function in the skin layer according to Eq. (2) (a self-similar solution of the kinetic equation with heat transfer ignored). The dashed line is a Maxwellian distribution with the same average energy; the dot-dashed line is the result of a numerical solution of Eqs. (5)–(8) with $\alpha = 0.5$, $\beta(0) = 0.5$, and $t = 83t_0$.

average electron energy in the skin layer (i.e., the temperature, since the electron distribution was assumed to be approximately Maxwellian in Ref. 7) increases as $t^{6/25}$:

$$\langle \epsilon_e \rangle \approx T_* = T_* (t/t_*)^{6/25}, \quad (3)$$

where T_* and t_* are characteristic parameters with the dimension of an energy and a time, given by

$$T_* = 0.77 mc^2 (v_{osc}/c)^{3/2} (\omega_0/\omega_p)^2, \quad (4)$$

$$t_* = 1.18 (mc^3 / Ze^4 n_e \Lambda) (v_{osc}/c)^{3/4} (\omega_0/\omega_p)^3.$$

Here $\omega_p = (4\pi e^2 n_e / m)^{1/2}$ is the electron plasma frequency, $v_{osc} = eE_0 / m\omega_0$ is the velocity amplitude of the electron oscillation in the vacuum electric field of the laser light, Z is the average degree of ionization, and Λ is the Coulomb logarithm, which appears in the expression for the rate of electron-ion collisions.

The depth l_i of the heated region increases considerably more rapidly than l_S :

$$l_S \propto t^{1/25}, \quad l_i \propto t^{4/5}.$$

2.2. Description of the kinetic model of the heat transfer

According to Refs. 1, 6, and 7, the interaction of laser pulses of subpicosecond length and high intensities ($I > 10^{17}$ W/cm²) occurs under conditions corresponding to the anomalous skin effect. In this case the assumption that the heat flux is classical is wrong near the absorption region, since the skin thickness is smaller than the electron mean free path under the conditions of the anomalous skin effect. To find a better description of the heat transfer out of the absorption region, we have carried out a numerical solution of the kinetic equation for the electron distribution function:

$$\frac{\partial f_e}{\partial t} + v_z \frac{\partial f_e}{\partial z} + \frac{e}{m} E_a(z, t) \frac{\partial f_e}{\partial v_z} = v_{ei} \frac{1}{\sin \varphi_v} \frac{\partial}{\partial \varphi_v} \left(\sin \varphi_v \frac{\partial f_e}{\partial \varphi_v} \right), \quad (5)$$

where

$$v_{ei} = 2\pi Ze^4 n_e \Lambda / m^2 v^3$$

is the rate of electron-ion collisions, and φ_v is the angle between the velocity vector v and the z axis.

Under anomalous-skin-effect conditions the electron mean free path is greater than the skin thickness. To avoid introducing this small length scale in the problem, we solve the kinetic equation (5) exclusively outside the skin layer. The absorption of the laser light is described as a boundary condition on the distribution function at the boundary $z = 0$:

$$\begin{aligned} [f_e] &\equiv f_e(v_z \geq 0, v_\perp, z=0, t) - f_e(v_z \leq 0, v_\perp, z=0, t) \\ &= 2 \frac{v_{osc}^2}{c^2} (\omega_0 l_s)^6 \frac{v_\perp^2}{v_z} \frac{\partial}{\partial v_z} \left[\frac{v_z \partial f_e / \partial v_z}{v_z^6 + (\omega_0 l_s)^6} \right]. \end{aligned} \quad (6)$$

The right side of (6) contains the distribution function of the electrons moving toward the boundary;

$$v_\perp = (v_x^2 + v_y^2)^{1/2}$$

is the velocity component in the plane of the interface; and the skin thickness is expressed self-consistently in terms of the distribution function, as in Refs. 6 and 7:

$$l_s(t) = \left(\frac{mc^2}{4\pi^3 e^2 \omega_0} \right)^{1/2} \left| \int_0^\infty d v_\perp \left(\frac{v_\perp^3}{v_z} \frac{\partial f_e}{\partial v_z} \right) \Big|_{v_z=0} \right|^{-1/2}. \quad (7)$$

A boundary condition of this sort was found previously, in Refs. 6 and 7 by solving the kinetic equation approximately inside the skin layer in the quasilinear approximation, with collisions ignored.¹⁾ Condition (6) causes a redistribution of the electrons with respect to transverse velocity, but it does not give rise to a current along the z axis.

The electron distribution function is assumed to be axisymmetric with respect to the normal to the surface (the z axis). The distribution function is assumed to depend only on the one coordinate z . These assumptions correspond to normal incidence of the laser light (which may be either unpolarized or circularly polarized) on a plane $z = 0$ boundary. The ions are assumed to be cold and immobile, with a fixed density $n_i = n_e / Z$.

An ambipolar electric field $E_a(z, t)$ arises in the plasma in order to maintain quasineutrality of the plasma. To determine this field we use the standard assumption that there is no electron current along the z axis:

$$\int d v_z f_e(v_z, v_\perp, z, t) = 0. \quad (8)$$

This assumption is valid for describing processes which are slow in comparison with the period of the plasma oscillations, $\approx \omega_p^{-1}$. This condition clearly holds in our case, since the characteristic plasma heating rate

$$\tau = (d \ln T / dt)^{-1}$$

is high in comparison with ω_0^{-1} , and the relation $\omega_0 \ll \omega_p$ holds. The boundary condition in (6) does not give rise to a current. We thus have $E_a(z = 0, t) = 0$ at the boundary. The field E_a arises because of collisions, which change the direction in which the electrons are moving and thus tend to make the distribution function isotropic.

Equation (5) incorporates only electron-ion collisions. Electron-electron collisions are ignored, under the assumption that the ionization state of the ions is large, $Z \gg 1$. The "Maxwellization" of the distribution function in the interior of the plasma is described formally by means of a boundary

condition for $f_e(v_z \leq 0, z \rightarrow \infty)$, which is assumed to be Maxwellian and isotropic.

The algorithm used for the numerical solution of Eqs. (5)–(8) is described in detail in the Appendix. At this point we simply note that the high dimensionality of the problem (there are two velocity components, v_\perp and v_z ; one coordinate, z ; and the time t) rules out the use of this code for calculations over large time or spatial intervals. In practice, the calculations were carried out over a distance on the order of ten mean free paths of a thermal electron, z_0 , and over times on the order of the mean free path t_0 multiplied by a few tens (up to a hundred). These intervals were too narrow to see the dynamics of the heating as the temperature changed by a factor of a few units or more.

To get around this difficulty we used the following tactic. Our problem, (5)–(8), has two independent parameters. It is convenient to adopt the intensity of the laser light as one of them; more precisely, we adopt the ratio of the electron oscillation energy in the field of the laser light to the rest energy of an electron, $\alpha = (v_{osc}/c)^2$. As the second parameter we adopt the coefficient $\beta = \omega_0 l_s / \langle v_z^2 \rangle^{1/2}$, which is a measure of the extent to which the situation is anomalous and characterizes the average electron energy (or the temperature). During heating caused by a laser pulse of constant intensity, the first parameter, α , remains constant, while the second, β , decreases.

To study the time evolution $\beta(t)$ at a fixed value of α , we carried out a series of relatively short calculations for a fixed value of α and various initial values of β . Each calculation at a certain $\beta = \beta_1$ was pursued for a comparatively short time, until a quasisteady distribution function was reached. We determined the quasisteady heating rate $\tau(T_1)$, the degree of anisotropy Δ , and certain other properties. Then, using a different value $\beta = \beta_2$ (and thus a different temperature T_2), we repeated the calculation, again determining the heating rate. As a result of this series of calculations we found a sequence of $\tau(T_j)$ values, which we were then able to use to get an idea of the functional dependence $\tau(T)$ and thus of the dynamics of the plasma heating.

2.3. Results of the numerical calculations

The calculations were carried out over an interval on the order of 5 or 10 mean free paths near the plasma boundary. We assumed that the distribution function was initially Maxwellian and isotropic with some given temperature T_0 . The boundary condition (6) was imposed at the left boundary (the plasma-vacuum boundary), and the condition of free outflow of heat was imposed at the right boundary (which was in the interior of the plasma). Specifically, it was assumed that electrons moving toward this right boundary escaped freely from the computation region, while electrons returned with a Maxwellian distribution with the same average energy and density, in such a way that there was no current of particles across the right boundary. (A boundary condition of this sort models electron-electron collisions in the interior of the plasma.)

As the unit of energy in the calculations we adopted the temperature of the initial Maxwellian distribution, T_0 . As the length and time scales, we used the electron mean free

path z_0 and the time scale between electron-ion collisions, t_0 , both calculated from the initial electron temperature:

$$z_0 = (T_0/m)^{1/2} / v_{ei}(T_0), \quad t_0 = v_{ei}^{-1}(T_0). \quad (9)$$

In the course of the calculations we determined the spatial and temporal behavior of the average electron energy in the longitudinal and transverse directions:

$$T_{\perp} = \frac{1}{2} \int d\mathbf{v} (m v_{\perp}^2 / 2) f_e, \quad T_z = \int d\mathbf{v} (m v_z^2 / 2) f_e. \quad (10)$$

We used these results to calculate the average electron energy

$$T(z) = \frac{1}{3} (T_z + 2T_{\perp}) \quad (11)$$

and the anisotropy parameter

$$\Delta = T_{\perp} / T_z - 1. \quad (12)$$

Calculations show that a quasisteady temperature profile and a quasisteady distribution function are formed over a time on the order of $(20-40)t_0$. Thereafter, the heating proceeds without any significant change in the shape of the distribution function or the temperature profile.

Figure 2 shows cross sections of the electron distribution function at several distances from the boundary. The lower half of these figures ($v_z < 0$) corresponds to electrons which are moving toward the boundary, and the upper half ($v_z > 0$) to those which are moving away from the boundary. We find the greatest difference between $f_e(v_z < 0)$ and $f_e(v_z > 0)$ near the boundary. This difference is a consequence of the anisotropy of the heating in the skin layer:

Electrons with small longitudinal velocities acquire energy from the field. Accordingly, the transverse electron energy T_{\perp} is greater than the longitudinal energy T_z near the boundary (Figs. 2 and 3). For the parameter values under consideration here, the anisotropy of the electron distribution is slight [$\Delta(z=0) \approx 0.1-0.2$] and depends only weakly on the time (Fig. 3). The anisotropy of the electron distribution may, as we will see below, lead to an increase in the absorption coefficient and to the excitation of an electromagnetic instability.¹⁹

With distance from the boundary, the electron distribution becomes more nearly isotropic (Fig. 3), and Δ decreases, because of electron-ion collisions. At $z \approx 5z_0$, traces of anisotropy remain only for the fastest electrons, with $v \approx 5(T_0/m)^{1/2}$. These electrons undergo essentially no collisions over the computation distance. The spatial dependences of $\Delta(z)$ remains essentially the same as time elapses. The implication is that the heating is quasisteady.

Figure 4 shows examples of the average plasma temperature T profile as a function of position [see (11)]. We see that the shape of the $T(z)$ profile does not change as time elapses; this result indicates that the heating is approximately self-similar. The length scale of the temperature variation,

$$L_t = (d \ln T / dz)^{-1}$$

is comparable to the electron mean free path near the boundary. We thus find $L_t \approx 7z_0$ at $z \approx 0$ from Fig. 4. However, the profile becomes more gently sloping even close to the boundary, and at $z \approx 6z_0$ we have $L_t \approx 60z_0$. This fact is evidence that the nonclassical heat transfer is manifested most notice-

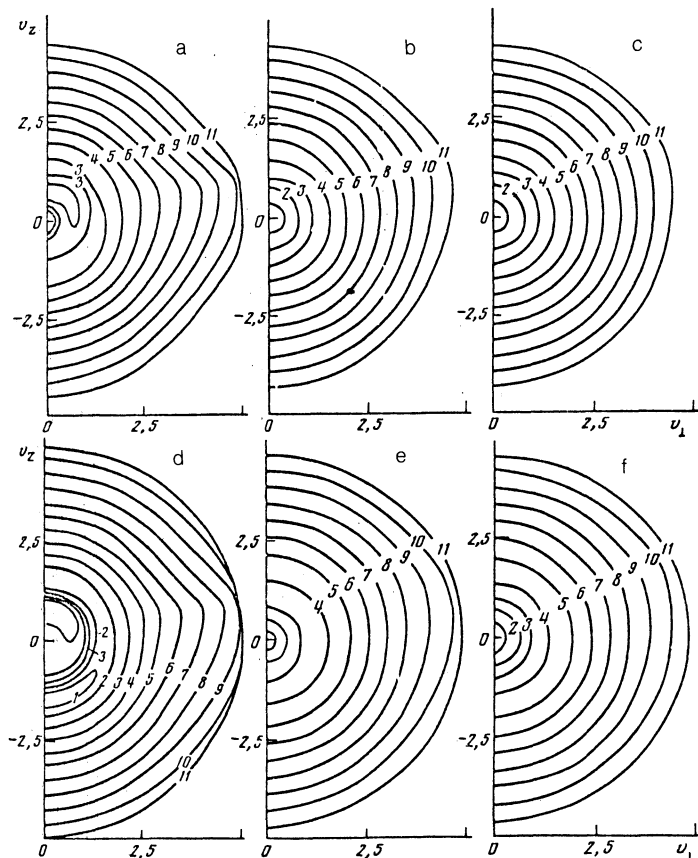


FIG. 2. Contour plots of the electron distribution function $f_e(v_{\perp}, v_z)$. a, d—Near the plasma boundary, $z \approx 0$; b, e—at a distance of three mean free paths, $z/z_0 = 3$; c, f—at a distance $z \approx 6z_0$. a, b, c) At the time $t = 10t_0$; d, e, f) $40t_0$. The parameter values $\alpha = 0.5$ and $\beta(0) = 0.75$ were used in the calculations. The labels i on the contour lines correspond to a value of the distribution function less than the maximum value by a factor of $\exp(3i/11)^2$ for each part of the figure.

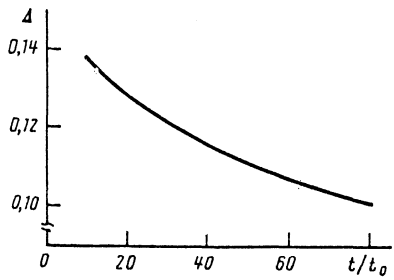


FIG. 3. Time evolution of the parameter which serves a measure of the anisotropy of the distribution function at the $z \approx 0$ boundary, i.e., $\Delta(t)$. The parameter values used in the calculations were the same as in Fig. 2.

ably near the boundary. At distances $z \approx 10z_0$ the classical description of the heat transfer becomes valid essentially everywhere except in a small region near the front of the thermal wave, where the temperature gradient again increases sharply. That region does not affect the plasma boundary, however, so we will not discuss it here.

The heating rate can be determined from Fig. 5. We see that at times $t \leq 20t_0$ a self-similar regime is formed, and the rate of increase of $T(0,t)$ is higher than at later times. The reason lies in a relaxation of the initial conditions, in particular, the circumstance that the temperature in the layer is initially more nearly uniform, and the distribution function is Maxwellian. A steady-state heating regime then sets in. In particular, for Fig. 5 [$\alpha = 1, \beta(0) = 0.75$] the time scale of the temperature changes is $\tau \approx 170t_0$, while at $\beta(0) = 1$ it is $\tau \approx 50t_0$. The heating rate thus falls off with increasing plasma temperature. The reason is that the heat flux out of the skin layer (which is comparable in magnitude to the free molecule heat flux) increases more rapidly than the absorption coefficient with increasing temperature.

To explicitly see the deviation from the classical thermal conductivity, we compare the results found in the present calculations with a self-similar solution carried out with the help of the classical thermal conductivity in (3). Figure 6 shows the plasma heating rate τ versus the temperature at the boundary, $T(0)$. According to (3), the classical thermal conductivity leads to $\tau \propto [T(0)]^{25/6}$. The results of kinetic calculations are shown in the same figure, by the points. As the temperature scale and the time scale we used expressions (4). At $T = T_*$, the anomaly parameter is $\beta(T_*) \approx 1$; i.e., T_* determines a lower boundary on the region of the anomalous skin effect. Correspondingly, the time scale t_* determines the heating rate τ_* at $T = T_*$ according to the classical theory.⁷

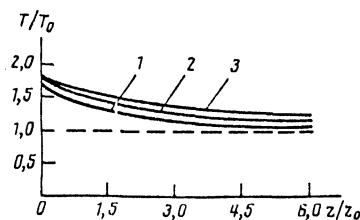


FIG. 4. Profile of the average electron energy $T(z)$ at various times: 1— $t = 10t_0$; 2— $20t_0$; 3— $40t_0$. The parameter values are the same as in Figs. 2 and 3.

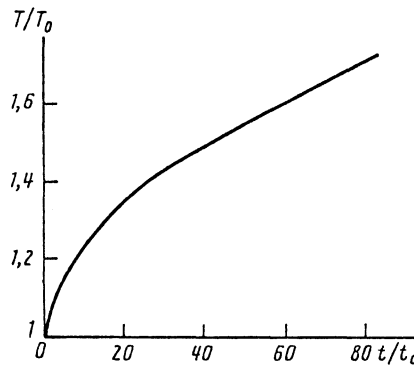


FIG. 5. Time evolution of average plasma temperature at the boundary, $T(0,t)$, for $\alpha = 0.5$ and $\beta(0) = 0.75$.

The kinetic calculations demonstrate an important difference between the heating rate and the classical self-similar solution. With decreasing β , i.e., with increasing temperature T , this difference becomes even greater. Although the data in Fig. 6 were obtained over a fairly narrow interval of parameter values, they can be approximated by

$$T \propto t^{0.4}. \quad (13)$$

This growth is considerably faster than that predicted by the classical theory of heat conduction:⁷ $T \propto t^{0.24}$.

Even near the boundary of the region of the anomalous skin effect, at $T \approx T_*$ ($\beta \approx 1$), the heating rate is greater than the classical rate by nearly an order of magnitude. This difference indicates that the deviation from the classical thermal conductivity may be significant even at lower temperatures, under conditions corresponding to the normal skin effect. Using the classical scaling for the temperature under the conditions of the normal effect,⁷ $T \propto t^{1/6}$, we would expect that anomalies would appear in the thermal conductivity.

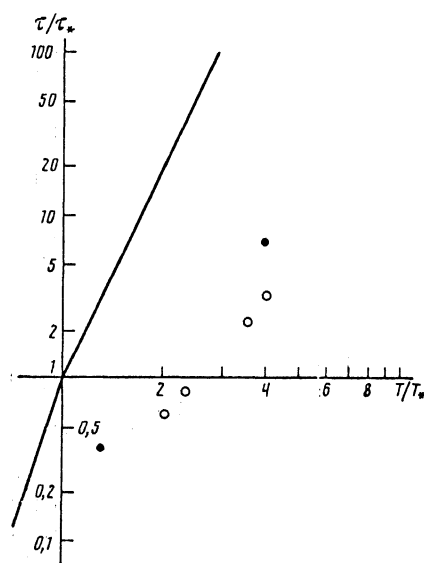


FIG. 6. Temperature dependence of the plasma heating rate under conditions corresponding to the anomalous skin effect. Solid line—Result of a self-similar solution under the assumption of a classical thermal conductivity, in accordance with (3) and (4); filled points—results of kinetic calculations with $\alpha = 0.5$; open circles—the same, with $\alpha = 0.25$.

ity, and the heating rate would rise correspondingly, at temperatures $T \approx (0.3-0.5) T_*$.

Heating of the plasma under anomalous skin-effect conditions leads to a distinctive shape of the electron distribution function near the boundary (Fig. 7). In comparison with a Maxwellian distribution, there are deficiencies of electrons with low and high velocities. In addition, a positive derivative $\partial f_e / \partial v_z$ appears. This fact suggests that ion acoustic and plasma waves may be excited and that an anomalous (turbulent) resistance arises.²⁰ We have not considered that effect in the present paper. It might lead to even greater suppression of the heat flux and, correspondingly, a heating rate greater than (13). The distribution function in Fig. 7 (see also Fig. 1) has qualitatively the same shape as the self-similar distribution function in (2), which was derived analytically in Ref. 6 by ignoring the heat loss from the skin layer and by assuming an isotropic distribution function. Although neither of these assumptions is strictly correct, there is indeed a deficiency of slow particles.

3. EFFECT OF AN ANISOTROPY OF THE ELECTRON DISTRIBUTION ON THE ABSORPTION OF ENERGY FROM A LASER PULSE UNDER CONDITIONS CORRESPONDING TO THE ANOMALOUS SKIN EFFECT

The numerical solution described above demonstrates the formation of an anisotropic, non-Maxwellian distribution near the plasma boundary. It is therefore interesting to take a separate look at how the absorption of laser energy depends on the shape of the electron distribution function.

The problem of energy absorption under anomalous skin-effect condition is described in detail in Refs. 8-11 for a distribution function which is specified, which remains constant over time (differing in these regards from the distribution function discussed in the preceding section of this paper), and which is otherwise arbitrary, and for the case of a monochromatic electromagnetic wave. Following the general theory, we can thus immediately write expressions for the absorption coefficient A for the energy flux for s - and p -polarized laser pulses:¹⁰

$$A_s = 1 - \left| \frac{\xi_s \cos \theta - 1}{\xi_s \cos \theta + 1} \right|^2, \quad A_p = 1 - \left| \frac{\xi_p - \cos \theta}{\xi_p + \cos \theta} \right|^2, \quad (14)$$

where θ is the angle of incidence of the light on the plasma, and ξ is the surface impedance. When laser light is applied to

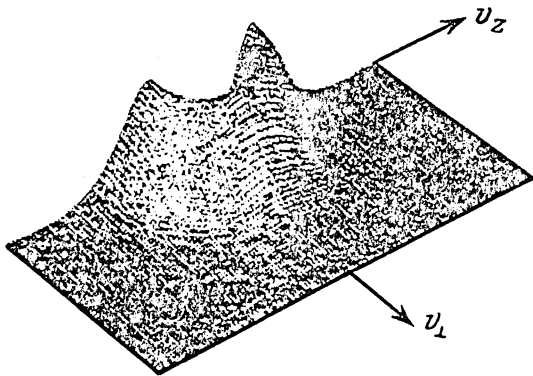


FIG. 7. Electron distribution with respect to longitudinal velocity v_z and with respect to transverse velocity v_1 near the plasma boundary, with $\alpha = 0.5$, $\beta(0) = 0.75$, and $t = 80t_0$.

targets with a smooth (polished) surface, it is natural to assume that the reflection of electrons from the surface is specular. According to Refs. 8-11, the relationship between the Fourier components of the field and the current in this case is the same as in an unbounded plasma. The surface impedances ξ_s and ξ_p (for s - and p -polarized waves, respectively) can therefore be written as integrals of components of the dielectric tensor of an unbounded plasma, $\epsilon_{ij}(\omega, \mathbf{k})$. We choose a coordinate system whose z axis runs along the normal to the surface, into the plasma, whose x axis lies in the plane of incidence of the laser wave, and whose y axis is perpendicular to this plane. For an s -polarized wave (in this case there are the magnetic field components B_x and B_z and the electric field component E_y) we then find¹⁰

$$\xi_s = \frac{E_y(0)}{B_x(0)} = -\frac{2ik}{\pi} \int_0^\infty \frac{dq}{q^2 + k^2 \sin^2 \theta - k^2}, \quad (15)$$

where

$$k = \omega_0/c, \quad \epsilon_{ij} = \epsilon_{ij}(\omega_0, \kappa \sin \theta, 0, q).$$

Correspondingly, for a p -polarized wave (with the field components E_x , E_z , and B_y), we find

$$\begin{aligned} \xi_p &= -\frac{E_x(0)}{B_y(0)} \\ &= -\frac{2ik}{\pi} \int_0^\infty \frac{dq}{q^2 - k^2 \epsilon_{xx} - (q \sin \theta + k \epsilon_{xz})^2 / (\sin^2 \theta - \epsilon_{zz})}. \end{aligned} \quad (16)$$

The problem of finding the absorption coefficient is thus reduced to one of determining the components of the dielectric tensor and of evaluating the integrals in (15) and (16). In a dense plasma ($n_e \gg n_c$), the impedance is small ($|\xi| \ll 1$), so we can replace (14) by the following simpler expressions for the absorption coefficients:

$$A_s \approx 4 \cos \theta \operatorname{Re} \xi_s, \quad A_p \approx 4 \cos^{-1} \theta \operatorname{Re} \xi_p. \quad (17)$$

The second of these expressions is valid everywhere except in a small angular interval near $\pi/2$, where we have $\cos \theta \approx |\xi_p|$, where A_p reaches a maximum, and where we should use the exact formula (14).

The same small parameter, $n_c/n_e \ll 1$, can be used to derive some comparatively simple expressions for the tensor components ϵ_{ij} . For this purpose we note that the components ϵ_{ij} are large: $|\epsilon| \approx n_e/n_c \gg 1$. The integrals in (15) and (16) are therefore dominated by large values of the z component of the wave vector: $q \approx q_* \approx k|\epsilon| \gg k$. The x component of the wave vector can thus be ignored in the arguments of ϵ_{ij} . (The physical meaning here is that the length scale of the field variations in the skin layer, l_s , is much smaller than the vacuum wavelength: $\omega_0 l_s/c \ll 1$.) The direction of the anisotropy axis of the distribution function thus essentially coincides with the direction of the wave vector.

We also note that under the conditions corresponding to the anomalous skin effect the field penetration depth $q_*^{-1} \approx l_s$ is short in comparison with the distance traveled by an electron over the field period, v_{tz}/ω_0 [where $v_{tz} = (T_z/m)^{1/2}$], and also in comparison with the mean free path of an electron, v_{tz}/v_{ei} . In the calculation of ϵ_{ij} we should thus set $|q|v_{tz} \gg \omega_0$. Expanding ϵ_{ij} in a series in

$\omega/|q|v_{tz}$, we find the following expressions for the impedance:

$$\xi_s = (\omega_0 l_s / \pi c) \Phi(d), \quad (18)$$

$$\xi_p = \xi_s + i \sin^2 \theta \left(-\frac{4\pi e^2 m c^2}{\omega_0^2} \int dp \frac{\gamma}{p_z} \frac{\partial f_0}{\partial p_z} \right)^{-1/2}, \quad (19)$$

$$\Phi(d) = 2 \int_0^\infty du u [1 + iu(u^2 - d)]^{-1}, \quad (20)$$

where the quantity $d = (\omega_p l_s / c)^2 \Delta$ is proportional to the anisotropy parameter Δ ,

$$\gamma = (1 + p^2 / m^2 c^2)^{1/2}$$

is the relativistic factor, and

$$\Delta = -\frac{1}{n_e} \int dp \left\{ \left[1 + \frac{p_z^2 + p_\perp^2 / 2}{m^2 c^2} \right] \gamma^{-3} f_0 + \frac{p_\perp^2}{2 p_z \gamma} \frac{\partial f_0}{\partial p_z} \right\}, \quad (21)$$

$$l_s = \left[-\frac{4\pi^3 \omega_0 e^2}{c^2} \int_0^\infty dp_\perp \left(\frac{p_\perp^2}{p_z} \frac{\partial f_0}{\partial p_z} \right) \Big|_{p_z=0} \right]^{-1/2}. \quad (22)$$

If relativistic effects are ignored, expression (22) for the skin depth becomes the expression (7) written above and expression (21) for the anisotropy parameter becomes the same as (12) for a nonrelativistic, two-temperature Maxwellian distribution.

The second term in (19) is smaller than the first by a factor of $(\omega_0 l_s / v_{tz})^{-1/2}$, so we have

$$\xi_p \approx \xi_s \equiv \xi.$$

The impedance ξ is small since the parameter $\omega_0 l_s / c \ll 1$ is small. The parameter $\omega_p l_s / c$ beside d in the expression for d in (20) may be greater than unity under the conditions of the anomalous skin effect. Consequently, even when the anisotropy parameter is small, $\Delta \ll 1$, the effect of this parameter on the impedance and thus on the absorption coefficient may be substantial.

The Δ dependence of the impedance is described by the function $\Phi(d)$ in (20); plots of the real and imaginary parts of this function are given in Fig. 8. With $d = 0$, the real part of the integral in (20) reduces to the tabulated value

$$\text{Re } \Phi(0) = 2\pi/3^{3/2} \approx 1.2.$$

The maximum value, $\text{Re } \Phi_{\text{max}} \approx 2.2$, however, is nearly twice as large as $\text{Re } \Phi(0)$, and it is reached at $d \approx 1.6$.

To illustrate the use of the general expressions given above, we consider a nonrelativistic, bi-Maxwellian distribution function:

$$f_e(v) = \frac{n_e m^{3/2}}{(2\pi T_z)^{1/2} 2\pi T_\perp} \exp\left(-m \frac{v_z^2}{2T_z} - m \frac{v_x^2 + v_y^2}{2T_\perp} \right). \quad (23)$$

In this case the anisotropy parameter is given by (12), and the skin depth in (22) is equal to

$$((\pi/2)^{1/2} \omega_p^2 \omega_0 T_\perp / c^2 v_{tz} T_z)^{-1/2}.$$

The absorption is described by the real part of the im-

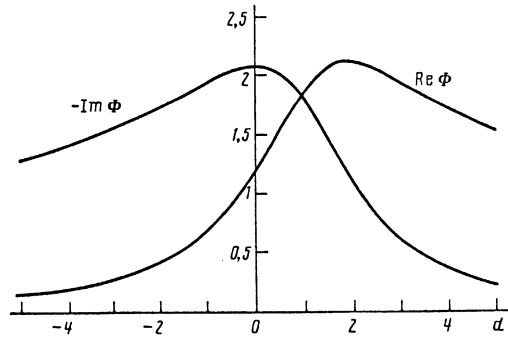


FIG. 8. Real and imaginary parts of the impedance versus the degree of anisotropy of the distribution function according to (20).

pedance and is correspondingly proportional to $\text{Re } \Phi$. It can be seen from Fig. 8 that for small values of Δ the absorption increases with increasing transverse temperature. It is just this situation which is realized under the conditions of the anomalous skin effect (as we showed in the preceding section of this paper), because of the preferential heating of electrons moving at small angles with respect to the surface.

Figure 8 shows angular distributions of the absorption coefficients. In accordance with (14) and (17), A_s falls off monotonically with increasing angle of incidence. The anisotropy of the distribution function does not change the shape of the $A_s(0)$ curve. For a p -polarized wave and a symmetric distribution function ($\Delta = 0$), the absorption maximum

$$A_{p \text{ max}} = 2 \text{Re } \xi / (\text{Re } \xi + |\xi|) \approx 2/3$$

is reached at the angle of incidence corresponding to

$$\cos \theta = |\xi|.$$

The anisotropy of the distribution function for $\Delta > 0$ leads to an increase in the maximum value of A_p , since the phase of the impedance decreases. The coordinate of the maximum shifts to a larger angle, since $|\xi|$ decreases. For $\Delta < 0$, the maximum of the absorption coefficient shrinks because of the increase in the phase of the impedance, but the maximum again shifts toward large values of θ because of the decrease in $|\xi|$. Note the narrowing of the A_p maximum with increasing degree of anisotropy of $|\Delta|$.

Note also that the difference between A_p and A_s stems from the work performed on the electrons by the longitudinal field component E_z . Correspondingly, for p -polarized light the absorption of energy arises from an increase in the z component of the electron velocity. We would thus expect the longitudinal temperature T_z to be higher than the transverse temperature T_\perp . According to Fig. 9, this inverse anisotropy (the inverse of that in the case of the s polarization) leads to some decrease in the absorption.

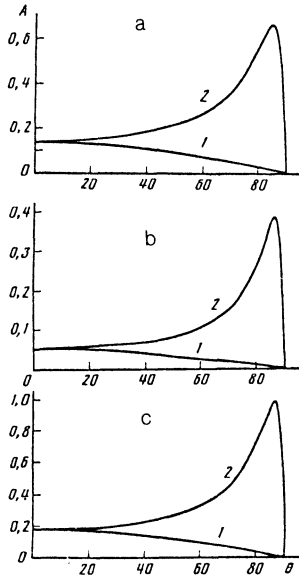


FIG. 9. Angular distribution of the absorption coefficient for (1) *s*-polarized and (2) *p*-polarized electromagnetic waves under conditions corresponding to the anomalous skin effect, with $n_e/n_c = 100$ and $v_{iz}/c = 0.1$. a—The value of the anisotropy parameter is $(\omega_p l_s/c)^2 \Delta = 0$; b— -2 ; c— -5 .

The behavior of the absorption of energy from a longitudinally polarized rf electric field near a sharp boundary of a dense plasma was discussed several years ago in Refs. 12 and 13. The absorption coefficient A_p found above for an isotropic distribution function agrees with the results of Ref. 12. The numerical simulation carried out by the particle-in-cell method in Ref. 13 showed that the absorption decreased somewhat as time elapsed, apparently because of the formation of an anisotropic distribution function.

4. CONCLUSION

We have discussed several effects which accompany the heating of a dense plasma by an intense, ultrashort laser pulse. It has been shown that at high intensities of the laser light (according to the scaling in Ref. 7, at intensities $I > 10^{17}$ W/cm², at a wavelength $\lambda \approx 0.25$ μ m, and at a pulse length $t_p \approx 100$ fs) we would expect several new effects to arise:

An increase in the plasma heating rate (and, correspondingly, an increase in the temperature), because of the limitation on the thermal conductivity and because of the transition from conditions corresponding to the normal skin effect to conditions corresponding to the anomalous skin effect;

The appearance of anisotropy of the electron distribution function in the skin layer as the result of the additional absorption and, possibly, a secondary instability;

The formation of a time-varying, nonequilibrium distribution function with deficiencies of slow and fast particles. The formation of a positive derivative of the electron distribution function ($\partial f_e/\partial v > 0$) may also be responsible for a secondary instability of the plasma, for the transition of the plasma to a turbulent state, for the appearance of an anomalous resistance, and for further suppression of heat transfer.

An important condition to be met for an experimental observation of these effects is the presence of a sharp plasma-vacuum boundary. For this purpose we need a high-quality target surface and a high-contrast laser pulse, to avoid the plasma production at the target surface before the arrival of the main laser pulse.

APPENDIX

Algorithm for solving the kinetic equation

1. Equation (5) can be written in the general form

$$\frac{Df}{Dt} = y^{-p} \frac{\partial}{\partial x} \left(a_{11} \frac{\partial f}{\partial x} + a_{12} \frac{\partial f}{\partial y} + a_1 f \right) + y^{-p} \frac{\partial}{\partial y} \left(a_{22} \frac{\partial f}{\partial y} + a_{12} \frac{\partial f}{\partial x} + a_2 f \right), \quad (\text{A1})$$

where $p = 1$, $x = v_z$, $y = v_\perp$ in the case of cylindrical coordinates in velocity space; or $p = 2$, $x = \cos\theta$, $y = |\mathbf{v}|$ in the case of spherical coordinates. The transport operator is, respectively,

$$\frac{Df}{Dt} = \frac{\partial f}{\partial t} + x \frac{\partial f}{\partial z} + E_a \frac{\partial f}{\partial x}, \quad p=1, \quad (\text{A2})$$

$$\frac{Df}{Dt} = \frac{\partial f}{\partial t} + xy \frac{\partial f}{\partial z} + E_a \left(x \frac{\partial f}{\partial y} + \frac{1-x^2}{y} \frac{\partial f}{\partial x} \right), \quad p=2,$$

where $E_a = E_a(z, t)$ is the ambipolar electric field. The coefficients in the collision operator [the right side of (A1)] may in general depend on the unknown distribution function, the time, and the phase variables.

Difficulties arise in attempts to numerically solve equations like (A1) by finite differencing, because the coefficients in the collision operator are rapidly varying functions in velocity space, because there are cross terms (mixed derivatives), and because it is necessary to carry out a multidimensional interpolation in phase space in calculating the result of the effect of the transport operator in each time step.

As computation time elapses, these circumstances may result in a buildup of numerical instabilities and errors. Below we discuss a numerical method for solving equations like (A1) which is based on a transformation to some special curvilinear coordinates, in which the collision operator has no mixed derivatives, and the transport operator is fairly simple. For the general case in which the coefficients in the collision operator depend on the time, these new curvilinear coordinates are dynamically related to the solution. They generate a mesh which adapts to the solution.

2. If we assume that the coefficients in (A1) are known functions of the phase coordinates at time t , then according to the theory of second-order particle differential equations a transformation

$$\xi = \xi(x, y), \quad \eta = \eta(x, y)$$

can put the right side of (A1) in canonical form, without any mixed derivatives. In general, however, this transformation may make the transport operator more complicated.

It is not difficult to verify that the switch to a form without mixed derivatives can be achieved by choosing only one function, e.g., $\xi = \xi(x, y)$, which determines one of the families of coordinate lines. The second function,

$\eta = \eta(x, y)$, can be determined independently, from (for example) the requirement that the transport operator Df/Dt be as simple as possible in form. In the case at hand we set $\eta \equiv y$.

To determine the function ξ , we associate with Eq. (A1) a first-order partial differential equation

$$a_{12}\partial\xi/\partial x + a_{22}\partial\xi/\partial y = 0.$$

For $a_{22} > 0$, this equation is equivalent to one ordinary differential equation for the coordinate lines:

$$dx/dy = a_{12}/a_{22}. \quad (\text{A3})$$

For definiteness, we choose the boundary conditions, which determine $\xi(x, y)$ unambiguously, in the form $\xi(x, y^*) = x$, where $y^* = \text{const}$.

This method for putting elliptic equations in a form without mixed derivatives is also much simpler than the standard method, in which one is obliged to deal with complex quantities and to determine two families of coordinate lines.

In the linear case, in which the coefficients a are independent of the time, Eq. (A1) in the coordinate system ξ, η determined in this manner is divergent, and it does not contain any mixed derivatives:

$$\eta^p \frac{\partial x}{\partial \xi} \frac{Df}{Dt} = \frac{\partial}{\partial \xi} \left(\tilde{a} \frac{\partial f}{\partial \xi} + \tilde{b} f \right) + \frac{\partial}{\partial \eta} \left[\frac{\partial x}{\partial \xi} \left(a_{22} \frac{\partial f}{\partial \eta} + a_2 f \right) \right], \quad (\text{A4})$$

where

$$\tilde{a} = (\partial\xi/\partial x) (a_{11} - a_{12}^2/a_{22}), \quad \tilde{b} = a_1 - a_2 a_{12}/a_{22}.$$

To calculate the effect of the collision operator in (A4) on each time layer, we construct an implicit, conservative, locally one-dimensional scheme in each time layer in the standard way.¹⁴

In the nonlinear case in which the coefficients in (A1) are time-varying, the curvilinear coordinates are dynamically related to the solution. They generate a mesh which adapts to the solution. Here there are two approaches which could be taken to construct a numerical scheme. If the coefficients a vary slowly in time (as they usually do for physical applications), one can convert the distribution function into an evolving coordinate mesh with an interval of a few time steps. When a different approach is taken, the partial derivative with respect to the time, $\partial f/\partial t$, in the transport operator takes the form

$$\partial f/\partial t - (\partial\xi/\partial x) (\partial x/\partial t) (\partial f/\partial t),$$

where $\partial f/\partial t$ now means^{15,16}

$$\partial f/\partial t|_{\xi, \eta = \text{const}}.$$

The appearance of the additional convective terms in this case is a consequence of the time variation of the coordinates ξ, η .

The latitude in the choice of coordinate systems here can be exploited for a variety of purposes. For example, if the particle transport under the influence of the operator Df/Dt is inconsequential, and if the inequalities

$$a_{11} \gg a_{12} \gg a_{22}$$

hold (i.e., if the momentum relaxation of the distribution function is much faster than the energy relaxation), then it would be natural to replace Eq. (A3) by the equation

$$dy/dx = a_{12}/a_{11}.$$

This generates the transformation

$$\xi(x, y), \quad \eta = x,$$

which sends the rays $x = \text{const}$ into themselves. After the equation is put in the form (A4), we can ignore the curvature of the coordinates because the ratio a_{12}/a_{11} is small. In other words, we can make the identification $\xi = y$. We then find a simplified equation in the original spherical coordinates:

$$\frac{\partial f}{\partial t} = y^{-2} \frac{\partial}{\partial x} \left(a_{11} \frac{\partial f}{\partial x} + a_1 f \right) + y^{-2} \frac{\partial}{\partial y} \left(\tilde{a} \frac{\partial f}{\partial y} + \tilde{b} f \right),$$

where we have $\tilde{a} = a_2 - a_{12}^2/a_{11}$, $\tilde{b} = a_2 - a_1 a_{12}/a_{11}$; and where a heating term $v^{-2} (\partial/\partial v) (a^* \partial f/\partial v)$ arises, where $a^* = v^2 (a_{vv} - a_{v\theta}^2/a_{\theta\theta})$. This term was derived previously in an averaged form by reducing the two-dimensional Fokker-Planck equations to simplified one-dimensional equations for a study of (for example) the heating of electrons.¹⁷

We thus see that, despite the large spread in the values of the coefficients of the highest derivatives, this method makes it possible to simplify the initial equations through an optimum choice of curvilinear coordinates.

3. It follows from (A2) that in the original cylindrical coordinates the transport operator is two-dimensional: It acts only along $y = \text{const}$ planes. For the numerical implementation of this operator, we need only a two-dimensional interpolation along the coordinates z and x . In spherical coordinates, in contrast, we need a three-dimensional interpolation, with a much faster change in the coefficients of the transport operator in phase space. In cylindrical coordinates, even in the simplest case in which there is only an angular diffusion [Eq. (5)], the collision operator has mixed derivatives. There are no such mixed derivatives in spherical coordinates.

When the method described above is applied to Eq. (5), we obtain a coordinate system consisting of a family of cylinders $v = \text{const}$ and planes $y = \text{const}$, $z = \text{const}$ (Fig. 10). In this coordinate system, Eq. (5) is

$$\begin{aligned} \frac{\partial f}{\partial t} \pm (v^2 - y^2)^{1/2} \frac{\partial f}{\partial z} \pm E(z, t) \left(1 - \left(\frac{y}{v} \right)^2 \right)^{1/2} \frac{\partial f}{\partial v} \\ = \frac{1}{yv} \left(1 - \left(\frac{y}{v} \right)^2 \right)^{1/2} \frac{\partial}{\partial y} \left[y \left(1 - \left(\frac{y}{v} \right)^2 \right)^{1/2} \frac{\partial f}{\partial y} \right]. \end{aligned} \quad (\text{A5})$$

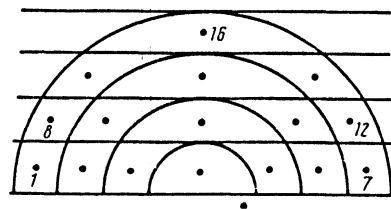


FIG. 10. System of curvilinear coordinates used in the numerical solution of the kinetic equation (5).

The \pm signs appear in (A5) because the mapping

$$(x, y) \rightarrow (v, y), \quad v = (x^2 + y^2)^{1/2}, \quad 0 \leq y \leq v$$

is double-valued. This double-valuedness does not pose any difficulties from the computational standpoint, since the distribution function can always be written in the form

$$f = f_+ + f_-,$$

where f_+ corresponds to particles which are moving away from the plasma boundary, and f_- to particles moving toward the boundary. Equation (A5) is therefore a shorthand version of a system of equations, in which the plus sign corresponds to f_+ , and the minus sign to f_- .

It can be seen from (A5) that in the coordinates v, y Eq. (5) has the fairly simple form of the transport operator corresponding to the case of cylindrical coordinates, and at the same time the simple form of a collision operator as in the case of spherical coordinates.

4. The method described above for solving Eq. (5) has been implemented in the *FP* numerical code. Let us describe it briefly. The volume element in the new coordinates is

$$Q = 2\pi v y (v^2 - y^2)^{-1/2} dy dv dz.$$

To avoid difficulties associated with the divergence of Q at $y = v$, we replace Q by the "exact" expression

$$\tilde{Q} = \frac{2}{3} \pi [(v_1^2 - y_2^2)^{3/2} + (v_2^2 - y_1^2)^{3/2} - (v_1^2 - y_1^2)^{3/2} - (v_2^2 - y_2^2)^{3/2}] dz,$$

where $(v_1, y_1), \dots, (v_2, y_2)$ are the nearest node coordinate points. It is a simple matter to verify that \tilde{Q} approximates Q within small terms of second order.

Using condition (8) and Eq. (5), we can determine the dimensionless ambipolar electric field from the formula

$$E_a(z, t) = [(\partial/\partial z) \langle v_z^2 \rangle + 2 \langle v_z/v^3 \rangle] / \langle 1 \rangle, \quad (\text{A6})$$

where $\langle \dots \rangle$ means averaging with the function f , and $v_z = \pm (v^2 - y^2)^{1/2}$.

The calculations show, however, that determining $E_a(z, t)$ on each time step from a formula of this sort results in the rapid development of a numerical instability associated with the uncertainty in $E_a(z, t)$ at $z = 0$ (at the boundary of the skin layer). According to (8), the meaning of the ambipolar electric field is that it supports a constant electron density and a zero average velocity along the z axis. In the *FP* numerical code, after calculating the effect of the diffusion and transport operators along z on each time step, we first normalize the distribution function in such a way that the dimensionless electron density is equal to one everywhere in the computation region. We then determine the average velocity along the v_z axis, i.e., u . We set

$$E_a(z, t) = -u/\Delta t,$$

where Δt is the time step. We calculate the result of the application of the operator

$$\partial f / \partial t \pm E_a(z, t) [1 - (y/v)^2]^{1/2} \partial f / \partial v = 0.$$

The calculations show that to two or three decimal places, the field determined in this manner is the same as the field found from (A6) everywhere except at $z = 0$.

The effect of the diffusion operator on the "flux" mesh (the points in Fig. 10) is evaluated by tridiagonal inversion, which is applied to the equation

$$\frac{\partial f}{\partial t} = \frac{1}{yv} \left[1 - \left(\frac{y}{v} \right)^2 \right]^{1/2} \frac{\partial}{\partial y} \left[y \left(1 - \left(\frac{y}{v} \right)^2 \right)^{1/2} \frac{\partial f}{\partial y} \right]$$

after this equation is approximated by a difference equation and after regularization of the expression $(v^2 - y^2)^{1/2}$ through the substitution

$$(v^2 - y^2)^{1/2} = 2\pi v y dy dv dz / \bar{Q}.$$

The quantity y takes on values from 0 up to v and back, corresponding to points between two neighboring semicircles in Fig. 10. The effect of the transport operators along z and v is calculated in succession by means of one-dimensional interpolations.

According to (6), direct modeling of the boundary condition at the point $z = 0$ generally also leads to the development of a numerical instability, because of the second derivative in the expression for the jump in the distribution function. In the numerical simulation of the boundary condition for the distribution function at the point $z = 0$, we accordingly carry out the following regularization: We replace f_e on the right side of (6) by a Maxwellian function

$$(2\pi\hat{T})^{-3/2} \exp(-v^2/2\hat{T}),$$

where the temperature \hat{T} is found from the instantaneous (not the Maxwellian) electron distribution function f_e^- at the point $z = 0$. Here we assume $f_e^- = f_e^+$ (only for this determination of \hat{T}).

For convenience in the calculations, the distribution function $f = f_{ij}$ is stored in an $n_2 \times n_2$ two-dimensional array, where $n_2 = n_v \times n_y$ ($n_v = n_y$). We first calculate arrays of the quantities \tilde{Q}_i , x_i , and y_i ($i = 1, \dots, n_2$). The scheme for numbering them is illustrated in Fig. 10 (for the particular case $n_2 = 16$). The calculation of the corresponding moments of f is carried out in the following way:

$$\langle 1 \rangle = \sum_{i=1}^{n_2} f_{i,j} \tilde{Q}_i, \quad \langle v_z \rangle = \sum_{i=1}^{n_2} f_{i,j} \tilde{Q}_i x_i.$$

$$T = \frac{1}{3} \langle v^2 \rangle = \frac{1}{3} \sum_{i=1}^{n_2} f_{i,j} \tilde{Q}_i (x_i^2 + y_i^2).$$

¹⁾ Equations (6) and (7) follow directly from expressions (19) and (20) of Ref. 6, but they are slightly different from Eq. (22) of Ref. 7. There, the effect of the magnetic field of the laser light on the motion of electrons in the skin layer was ignored.

¹⁾ E. G. Gamaliĭ and V. T. Tikhonchuk, Pis'ma Zh. Eksp. Teor. Fiz. **48**, 413 (1988) [JETP Lett. **48**, 453 (1988)].

²⁾ H. M. Milchberg and R. R. Freeman, Phys. Fluids B **2**, 1395 (1990).

³⁾ R. Fedosejevs, R. Ottmann, R. Sigel, G. Kuhnle, S. Szatmari, and F. P. Schafer, Phys. Rev. Lett. **64**, 1250 (1990); Appl. Phys. B **50**, 79 (1990).

⁴⁾ M. Chaker, J. C. Kieffer, J. P. Matte, H. Pepin, P. Andeberg, P. Maine, D. Strickland, P. Bado, and G. Mourou, Phys. Fluids B **3**, 167 (1991).

⁵⁾ C. H. Nam, W. Tighe, E. Valeo, and S. Suchewer, Appl. Phys. B **50**, 275 (1990).

⁶⁾ E. G. Gamaly, A. E. Kiselev, and V. T. Tikhonchuk, J. Sov. Laser. Res. **11**, 277 (1990).

- ⁷ W. Rozmus and V. T. Tikhonchuk, *Phys. Rev. A* **42**, 7401 (1990).
- ⁸ V. P. Silin and A. A. Rukhadze, *Electromagnetic Properties of Plasmas and Plasma-Like Media*, Gosatomizdat, Moscow, 1961.
- ⁹ E. M. Lifshitz and L. P. Pitaevskii, *Physical Kinetics*, Nauka, Moscow, 1979 (Pergamon, Oxford, 1981).
- ¹⁰ A. N. Kondratenko, *Penetration of a Field into a Plasma*, Nauka, Moscow, 1979.
- ¹¹ A. F. Alexandrov, L. S. Bogdankevich, and A. A. Rukhadze, *Principles of Plasma Electrodynamics*, Springer, New York (1984).
- ¹² F. Brunel, *Phys. Rev. Lett.* **59**, 52 (1987).
- ¹³ F. Brunel, *Phys. Fluids* **31**, 2714 (1988).
- ¹⁴ V. N. Novikov, *ZhVMiMF* No. 6, 920 (1990).
- ¹⁵ J. F. Thompson, Z. U. A. Warsi, and C. W. Mastin, *J. Comput. Phys.* **47**, 1 (1982).
- ¹⁶ P. A. Gnoffo, *AIAA J.* **21**, 1249 (1983).
- ¹⁷ V. Yu. Bychenkov, V. N. Novikov, V. P. Silin, and S. A. Uryupin, *Fiz. Plazmy* **17**, 418 (1991) [*Sov. J. Plasma Phys.* **17**, 244 (1991)].
- ¹⁸ E. G. Gamaly, V. T. Tikhonchuk, and A. E. Kiselev, *SPIE Proceedings*, Los Angeles, 1991.
- ¹⁹ E. S. Weibel, *Phys. Rev. Lett.* **2**, 83 (1959).
- ²⁰ V. Yu. Bychenkov, V. P. Silin, and S. A. Uryupin, *Phys. Rep.* **164**, 119 (1988).

Translated by D. Parsons